Physical properties of FeRh alloys: The antiferromagnetic to ferromagnetic transition

J. Kudrnovský and V. Drchal
Institute of Physics, Academy of Sciences of the Czech Republic, Na Slovance 2, CZ-182 21 Praha 8, Czech Republic

I. Turek
Faculty of Mathematics and Physics, Department of Condensed Matter Physics, Charles University, Ke Karlovu 5, CZ-12116 Praha 2, Czech Republic

(Received 14 November 2014; revised manuscript received 14 January 2015; published 29 January 2015)

The electronic, magnetic, thermodynamical, and transport properties of FeRh alloys are studied from first principles. We present a unified approach to the phase stability, an estimate of exchange interactions in various magnetic phases, and transport properties including the effect of temperature which are all based on the same electronic-structure model. Emphasis is put on the transition between the ferromagnetic (FM) and antiferromagnetic (AFM) phases. Such a study is motivated by a recent suggestion of FeRh as a room-temperature antiferromagnetic memory resistor. The theory predicts the order-disorder transformation from the hypothetical disordered bcc phase into ordered B2 phase. Comparison of exchange interactions in the magnetically ordered FM and AFM phases with corresponding spin-disordered counterparts allows us to identify relevant interactions which are precursors of magnetically ordered phases. The most important result is the explanation of a dramatic decrease of the resistivity accompanying the AFM to FM phase transition which is due to the spin disorder present in the system. The study of the anisotropic magnetoresistance in the AFM phase found recently experimentally is extended also to finite temperatures.

DOI: 10.1103/PhysRevB.91.014435 PACS number(s): 71.20.Be, 71.70.Gm, 72.25.Ba, 74.62.−c

I. INTRODUCTION

Equilibrium solid phases of the binary Fe-Rh system exhibit geometric structures related to the body-centered-cubic (bcc) and face-centered-cubic (fcc) lattices [1]. For alloys near the equiconcentration composition, the first phase below the melting point ($T_m = 1870$ K) is a fcc substitutional solid solution. Its cooling leads to a structural phase transition into a bcc-based B2-ordered (CsCl-type) FeRh alloy at temperature around 1570 K. This fact means that a hypothetical order-disorder phase transition on the bcc lattice takes place at a higher critical temperature $T_{\mathrm{ord}} > 1570$ K. After further cooling of the ordered FeRh alloy down to much lower temperatures, a transition from the paramagnetic state into the ferromagnetic (FM) state occurs at about $T_c = 670$ K (Curie temperature). Finally, the ferromagnetic phase transforms into the antiferromagnetic (AFM) phase at temperatures around $T_n = 370$ K which, however, can depend on the sample preparation [2]. It should be noted that the above-mentioned FM to AFM transition is reversible and can be realized either through the conventional temperature cooling/heating of the sample or with the help of external magnetic field applied to the AFM phase at temperatures close to but below the transition temperature to the FM phase. The release of the field (magnetic cooling) turns the FM phase back into the ground-state AFM phase. The reversibility of the FM to AFM transition was used recently to propose FeRh as a room-temperature antiferromagnetic memory resistor [3].

The electronic-structure properties of FeRh alloys have been a subject of numerous studies based on the density functional theory [4–9], although to give a comprehensive list is beyond the scope of this paper. The physical origin of the FM to AFM transition itself is still under debate (see, e.g., Refs. [10–15]). All these papers, however, agree on the decisive role played by Rh moments for this phase transition. This fact can be conveniently illustrated by a detailed study of exchange interactions in various magnetic phases of the FeRh alloy. Another consequence of the FM to AFM transition is a large drop of the resistivity ρ in the FM phase as compared to the AFM state, while the absolute value of ρ often depends on the sample preparation and the type of phase transition, namely, if it is induced by the temperature or by external magnetic field [16,17]. The large change of resistivities at the AFM to FM transition induced by applied external magnetic field allows us to speak about the large magnetoresistance effect during such transition. Specifically, the resistivity drops from about 125 $\mu\Omega$ cm in the AFM phase to about 65 $\mu\Omega$ cm in the FM state [16], giving thus the magnetoresistance larger than 50%. It should be noted that such magnetoresistance is much larger as compared to the conventional anisotropic magnetoresistance (AMR) which is induced by the relativistic effects and which exists in both the FM and AFM phases [3].

Motivated by the relevance of the FM to the AFM transition for the room-temperature AFM resistor [3], we have studied here various related physical properties of the FeRh alloy using a unified electronic-structure model in the framework of the local density approximation. We thus avoid the use of individually tailored inputs for different physical quantities. The following properties are studied: (i) the densities of states and magnetic moments in different magnetic phases as well as the study of the dependence of Rh moments on the canting angle θ between Fe and Rh moments (the latter study can describe the AFM to FM transition induced by an external field); (ii) the relevance of the Fe-Rh hybridization for the formation of Rh moment in the FM phase will be demonstrated by performing calculations with the switched-off spin-dependent part of the exchange-correlation potential on Rh atoms; (iii) the order-disorder transition from the

hypothetical disordered bcc $Fe_{0.5}Rh_{0.5}$ to the ordered B2 FeRh alloy and an estimate of corresponding T_{ord} using the generalized perturbation (GPM) and concentration-wave methods [18,19]; (iv) the exchange interactions based on the mapping to the classical Heisenberg Hamiltonian [20,21] and corresponding to various magnetic phases; (v) transport properties (residual resistivities) in both the FM and AFM phases using the linear-response theory (Kubo-Greeenwood approach) [22,23]. We investigate resistivities due to either a slight off-stoichiometry (Rh-rich FeRh alloy) or by using the finite-relaxation-time model applied to the ordered FeRh alloy and the existence of the AMR effect in the AFM state [3]; and (vi) the large drop of the sample resistivity during the AFM to FM transition mediated by the external magnetic field. This drop is due to the temperature-induced spin disorder and we employ the disordered local moment (DLM) approach and its variants [24] to study it. In all cases, we compare results of theoretical simulations with available experimental data.

II. FORMALISM AND COMPUTATIONAL DETAILS

The electronic-structure calculations were performed using the relativistic tight-binding linear muffin-tin orbital (TB-LMTO) method [23,25] within the local density approximation (LDA). In chosen cases, also the scalar-relativistic version of the TB-LMTO method [26,27] was employed like, e.g., in the study of the alloy phase stability and magnetic interactions. The Vosko-Wilk-Nusair exchange-correlation potential [28] was used for the parametrization of the local density functional. A possible effect of disorder is described by the coherent-potential approximation (CPA) as formulated in the framework of the TB-LMTO Green's function method [27]. The same atomic sphere radii were used for all constituent atoms, the lattice constant was taken from the experiment, and the s,p,d basis was used. We have verified that the electronic structure is modified only marginally when using the s,p,d,f basis. The disordered FeRh phase has the bcc structure, the FM FeRh phase adopts the B2, or the CsCl lattice type, and the AFM phase is the so-called AFMII one [4] characterized by alternating Fe↑-Rh-Fe↓-Rh layers along the [111] direction. The AFMII is thus formally equivalent to the Heusler alloy in which four interpenetrating fcc lattices are mutually shifted by the vector $a(1,1,1)/4$ (a is the lattice constant) and occupied, respectively, by Rh, Fe↑, Rh, and Fe↓ atoms ($L2_1$-$Rh_2Fe\uparrow Fe\downarrow$ Heusler alloy). It should be noted that for Fe sublattices occupied by Fe atoms with parallel moments we recover the B2-type structure, but with the halved lattice constant as compared to the AFMII lattice. All calculations, even for bcc and B2 phases, were done using the reference AFMII lattice for computational consistency.

The phase stability of the alloy A_xB_{1-x} is described by the Ising alloy Hamiltonian

$$H^{\mathrm{I}} = \sum_{i \neq j} V_{ij}\, \eta_i\, \eta_j\,, \tag{1}$$

where i,j are site indices, η_i is the occupation index which is one if the site i is occupied by atom A and zero otherwise. The quantities V_{ij} are the effective pair (chemical) interactions. The effective pair interactions V_{ij} are determined using the generalized perturbation method of Ducastelle [18] and defined in terms of the chemical pair interactions $V_{ij}^{Q,Q'}$ (Q,Q'= Fe or Rh) as

$$V_{ij} = V_{ij}^{\mathrm{Fe,Fe}} + V_{ij}^{\mathrm{Rh,Rh}} - V_{ij}^{\mathrm{Fe,Rh}} - V_{ij}^{\mathrm{Rh,Fe}}\,. \tag{2}$$

It should be noted that V_{ij} can depend on the presence of magnetic moments [19]. The positive/negative values of effective pair interactions indicate the tendency to prefer unequal/similar atom pairs in the alloy (ordering/segregation). In the GPM approach, one estimates chemical interactions from the high-temperature phase, namely, from the disordered bcc-($Fe_{0.5}$,$Rh_{0.5}$) in the present case. For completeness, we mention that an alternative Connolly-Williams approach extracts chemical interactions from possible low-temperature ordered alloy structures [29] rather than from a high-temperature disordered phase as in the GPM method.

The magnetic structure is described by the classical Heisenberg Hamiltonian

$$H^{\mathrm{H}} = -\sum_{i \neq j} J_{ij}\, \mathbf{e}_i \cdot \mathbf{e}_j\,. \tag{3}$$

Here, i,j are again site indices, $\mathbf{e}_i$ is the unit vector in the direction of the local magnetic moment at site i, and the quantities J_{ij} are exchange integrals between sites i and j. The exchange integrals J_{ij} are determined using the method of infinitesimal rotations of Liechtenstein [20], and its implementation within the present TB-LMTO method can be found in Ref. [21]. The exchange integrals, by construction, contain magnitudes of magnetic moments of atoms and their positive (negative) signs indicate a tendency to the FM (AFM) coupling.

The exchange integrals are conventionally determined using the reference FM state [13,20], but also other reference states can be used to derive them, e.g., the AFM state for the corresponding magnetic phase. It should be noted, however, that both the FM and AFM reference states already assume a specific magnetic order derived from the experiment. In order to gain a deeper understanding of the character of interactions, we will also estimate exchange integrals from the reference state with no prescribed magnetic order, i.e., from the paramagnetic state above the critical temperature which will be described here by the DLM reference state [24]. Finally, to see a possible effect of the nearest-neighbor environment, we also compare exchange integrals for the ordered (B2-FeRh) alloy with its disordered bcc-($Fe_{0.5}$,$Rh_{0.5}$) counterpart.

The residual resistivities are determined by the linear-response theory as formulated in the framework of the relativistic TB-LMTO-CPA method and its Kubo-Greenwood counterpart [23] including the disorder-induced vertex corrections [22,23]. The disorder-induced vertex corrections are equivalent to the backward scattering in the collision term of the Boltzmann transport theory.

The diagonal elements of the conductivity tensor read as

$$\sigma_{\mu\mu} \propto \mathrm{Tr}\,\langle v_\mu (g_+ - g_-) v_\mu (g_+ - g_-)\rangle, \tag{4}$$

where the Green's functions $g_\pm = g(E_{\mathrm{F}} \pm i\mathrm{Im}z)$ are obtained from self-consistent electronic-structure calculations, E_{F} is the Fermi energy, and Imz is its imaginary part, v_μ holds for a nonrandom operator describing hopping between various sites (the effective velocity in the intersite transport), and $\langle \ldots \rangle$

denotes the configurational averaging over the chemical or magnetic disorders. We refer the reader to Refs. [22,23,30] for details concerning formulation of the transport in the framework of the present relativistic TB-LMTO-CPA theory. The diagonal elements of the resistivity tensor $\rho_{\mu\mu}$ ($\mu = x,y,z$) are obtained by neglecting small off-diagonal elements of the conductivity tensor as $\rho_{\mu\mu} = 1/\sigma_{\mu\mu}$. It should be noted that the off-diagonal elements of the conductivity tensor are relevant, e.g., for the anomalous Hall effect which, however, is not the subject of this study. The residual resistivity ρ and the AMR ratio r^{AMR} are then obtained from calculated $\rho_{\mu\mu}$ values as

$$\rho = (2\rho_{xx} + \rho_{zz})/3, \quad r^{\mathrm{AMR}} = (\rho_{zz} - \rho_{xx})/\rho\,. \qquad (5)$$

In the present formulation, the magnetization points in the z direction.

The effect of temperature on transport properties has been studied using two approaches: (i) We employ the finite-relaxation-time model [3,31] in which temperature-dependent scatterings due to phonons and magnons (and, eventually, also due to chemical disorder) are modeled in a phenomenological manner by adding a finite imaginary part Imz to the Fermi energy entering corresponding Green's functions. It should be noted that in conventional transport calculations we employ Im$z = 10^{-5}$ Ry which corresponds to a fraction of $\mu\Omega\,\mathrm{cm}$ for metallic systems. This model can be used even for the ideal B2-FeRh alloy without chemical disorder. On the other hand, a relation of Imz and corresponding temperature is beyond the limits of this simple model; and (ii) the effect of spin disorder mediated by a finite temperature on transport properties will be studied using the uncompensated DLM model [32–34] (see Sec. III D 2). In this case, we employ a slightly off-stoichiometric Rh-rich FeRh alloy which is compatible with the experiment [3] although this model can be applied to ideal systems as well.

In this paper, we wish to investigate primarily the transport properties of FeRh alloys. The transport properties are, however, closely related to the corresponding electronic structure. Therefore, an agreement of various calculated physical properties based on the same electronic-structure model will give a better justification also to related transport properties. We will therefore start the discussion with basic electronic-structure properties (densities of states and magnetic moments) of different phases for which transport properties are estimated (the FM, AFM, or DLM), then continue naturally with the alloy phase stability, then with the study of the character of magnetic interactions which will allow a deeper understanding of the character of magnetic phases relevant for the transport, and finish finally with transport properties itself including an approximate study of their dependence on the temperature. During evaluation of different physical properties, various kinds of the disorder are present in studied system treated using the CPA. For the reader's convenience, we briefly summarize them as follows: (i) The chemical disorder present in disordered bcc-$Fe_{0.5}Rh_{0.5}$ will be used in the study of its alloy phase stability and/or to estimate the effect of local environment on exchange integrals (disordered and ordered phases have different local site occupation). (ii) The native chemical disorder present in the off-stoichiometric Rh-rich FeRh samples will be used in the AMR transport studies. (iii) The spin disorder present in the alloy at finite temperatures is a relevant source of the sample resistivity close to the critical temperatures. It can be also mapped approximately into a special type of the chemical disorder in the framework of the uncompensated DLM model. (iv) Finally, in some cases different types of disorder can be present in the studied system at the same time, e.g., in the case of the transport properties at finite temperatures where the above-mentioned native chemical disorder as well as the spin disorder due to temperature coexist.

III. RESULTS AND DISCUSSION

In this section, we present theoretical estimates of various physical quantities related to the FeRh alloy and compare them with available experimental data.

A. Electronic structure

1. *Densities of states and magnetic moments*

The total and atom-resolved local densities of states (DOS) for various phases, namely, for the nonmagnetic and FM ones in the ordered B2 structure and the AFMII and DLM (or paramagnetic) phases, are shown in Fig. 1. Calculations were done scalar relativistically. The following remarks are made: (i) Large local Fe and Rh DOS at the Fermi energy in the nonmagnetic phase are signatures of the instability of this phase towards the ferromagnetism (the Stoner criterion). (ii) The larger Fe DOS(E_{F}) as compared to the Rh one indicates larger local magnetic moment of Fe atoms (see following). (iii) Both the AFM and DLM phases have the zero total magnetic moment (corresponding total majority and minority DOS's are the same). The DLM DOS is smoothed out by the spin-disorder as the DLM phase corresponds formally to the equiconcentration ($Fe^{[+]}_{0.5}$,$Fe^{[-]}_{0.5}$)Rh alloy of oppositely oriented moments [24]. It describes formally a high-temperature paramagnetic phase. In both the AFMII and DLM phases, local Rh moments collapse to zero. There is a good agreement with corresponding DOS's obtained in a recent study [13].

Calculated scalar-relativistic local Fe moments in all phases are large, about $3\mu_{\mathrm{B}}$. Specifically, $m^{\mathrm{Fe}} = 3.023/\pm 2.955/\pm 2.932\mu_{\mathrm{B}}$ for the FM/AFMII/DLM phases, respectively. The local Rh moment in the FM phase is $m^{\mathrm{Rh}} = 1.184\mu_{\mathrm{B}}$ and zero in the AFMII and DLM phases.

For a comparison, we also show local moments obtained using the relativistic theory. Corresponding Fe spin moments for the FM/AFMII/DLM phases are almost the same, namely, $m^{\mathrm{Fe}} = 3.075/\pm 3.020/\pm 3.025\mu_{\mathrm{B}}$, respectively. The local spin Rh moments are $m^{\mathrm{Rh}} = 1.173\mu_{\mathrm{B}}$ for the FM state and zero for the AFMII and DLM phases. These results, of course, agree well with other calculations (see, e.g., Refs. [4,13]). The above results clearly show the relevance of Rh moments for the FM phase as contrasted with the AFMII/DLM phases with zero local Rh moments.

2. *Constrained calculations*

It is thus obvious that the values of Rh moments vary dramatically at the FM to AFM transition. We will further investigate this point by performing constrained noncollinear

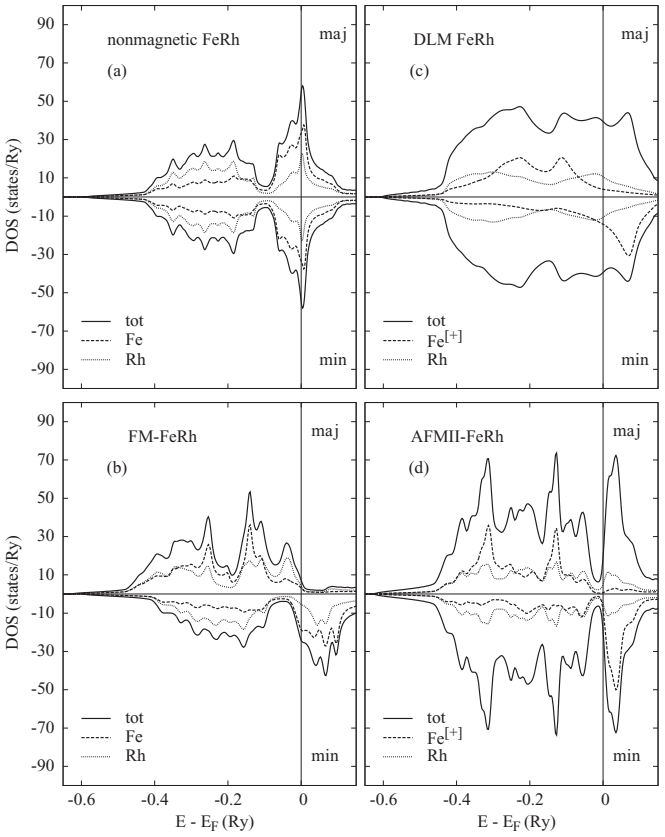

FIG. 1. The total and local densities of states for various phases: (a) the nonmagnetic B2-FeRh; (b) the FM B2-FeRh; (c) the DLM FeRh in the AFMII lattice; and (d) the ordered AFMII FeRh lattice. The DOS are resolved into the majority (maj) and minority (min) contributions while E_F denotes the Fermi energy. The majority and minority contributions are shown for one spin-orientation for the AFMII and DLM FeRh phases, for the other spin orientation the role of the majority and minority spins is interchanged. Note that the AFMII and CsCl lattices have different formula units containing, respectively, four and two atoms which are reflected in the area under the total DOS's, while the local DOS are normalized equally irrespective of the formula unit.

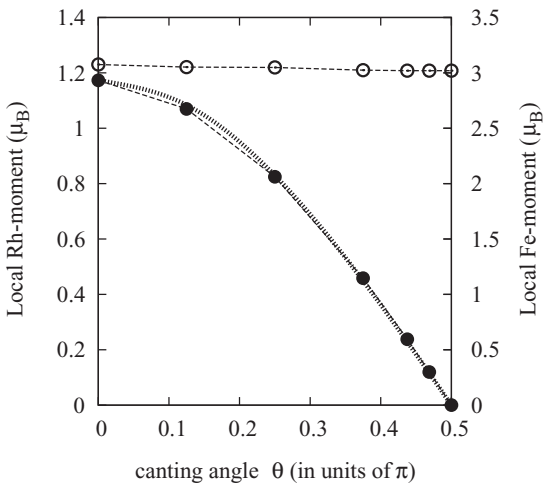

FIG. 2. The constrained noncollinear calculations assuming variation of the canting angle θ between magnetizations of Fe and Rh sublattices in the AFMII phase. The Rh moment (filled circles) points in the direction of the z axis, while the sublattice Fe moments (empty circles) are canted by an angle $\pm\theta$. The dotted line shows results of non-self-consistent calculations assuming a simple cosine form, namely, $m^{\mathrm{Rh}}(\theta) = m^{\mathrm{Rh}}(\theta = 0)\cos(\theta)$. The values $\theta = 0$ and $\pi/2$ correspond to the collinear FM and AFMII phases, respectively.

calculations in the AFMII phase. Specifically, the Rh moment is constrained to the z direction and we will vary the angle θ between moments on the Rh and Fe sublattices from 0 to $\pm\pi/2$. For $\theta = 0$, we recover the FM B2 phase (in a doubled unit cell) while for $\theta = \pi/2$ on one sublattice and $\theta = -\pi/2$ on the other one we have the AFMII phase. The present model is thus related to the FM-AFMII phase transition mediated by the external magnetic field (magnetic cooling or heating) [17]. Similar constrained calculations using the spin-spiral approach have appeared recently [13]. This reciprocal space approach is, however, limited to the ordered case and the scalar-relativistic limit. On the contrary, the present approach [23] is local and fully relativistic. In both cases, the local Fe and Rh moments are calculated self-consistently for each angle θ. It should be noted that we are not, however, able to relate the canting angle θ and the strength of applied magnetic field.

The transition between the AFMII and FM phases, which is due to switching of the external magnetic field, can be thus viewed as a gradual aligning of Fe spins on their sublattices accompanied by an increase of the Rh moment from its zero value in the AFMII phase to a finite Rh moment in the FM phase in which Fe spins on both Fe sublattices become parallel to each other. The resulting magnetic structure is thus changed from the parent AFMII lattice to the B2-type lattice in the FM phase. This process is reversible: gradual switching off the external field allows the system to return back to the AFMII phase which is the ground state with a lower energy. This picture is simplified because experimentally the AFM to FM transition occurs at a fixed temperature below the Curie temperature. In such case, a certain amount of the spin disorder already exists in the system. One can thus imagine a modified picture in which spin directions fluctuate around the statistically averaged value $\langle\theta\rangle$ of the canting angle which can be deduced, e.g., from the corresponding spin-spin correlation function obtained from the Heisenberg Hamiltonian based on the same electronic-structure model.

The result is shown in Fig. 2 for a system without spin disorder. We see that local Fe moments are rigid with respect to the canting angle θ as contrasted to local Rh moments whose sizes decrease with increasing angle between sublattice magnetizations and are zero for the canting angle $\theta = \pm\pi/2$ (the AFMII phase). It should be mentioned that the total energy of the AFMII state is lower than that of the FM state. The variation of the Rh moment as a function of the canting angle has a simple cosine form to a good approximation. The Fe moment is thus a good spin in the Heisenberg sense as contrasted to the non-Heisenberg behavior of the Rh moment. A detailed statistical study of the FeRh alloy should take this fact into account (see, e.g., Refs. [12,13]).

3. Neglect of exchange-correlation enhancement on Rh atoms

The relevance of the Fe-Rh hybridization for the occurrence of Rh moments in the FM state is generally accepted (see, e.g., Ref. [13] for extensive discussion on this point). Here, we wish to present another view of this problem. In metals, such as e.g., bcc-Fe, it is the spin-dependent part of the exchange-correlation potential which is responsible for its ferromagnetism. The Rh crystal is under ambient conditions nonmagnetic and its magnetism in the FeRh alloy is induced by moments on adjoining Fe atoms. Here, we wish to quantify which part of the Rh moment is due to the Fe-Rh hybridization alone and which part can be ascribed to the exchange part of the Rh potential. We thus calculate the Rh moment in the FM FeRh by explicitly switching off the spin-dependent part of the exchange-correlation potential on Rh atoms. The calculated spin polarization on Rh atoms is then the net effect of the hybridization of Rh atoms with Fe ones and their magnetic moments. A similar approach, although in a different context of the interlayer exchange coupling in Fe|Cr|Fe trilayers, was used in Ref. [35]. To illustrate the point it is enough to use the scalar-relativistic case although similar study can be done also in the fully relativistic case. We have obtained $m^{\mathrm{Fe}} = 2.939\mu_{\mathrm{B}}$ which compares very well with the result of the conventional case ($3.023\mu_{\mathrm{B}}$). The calculated $m^{\mathrm{Rh}} = 0.777\mu_{\mathrm{B}}$ should be compared to the value of $1.184\ \mu_{\mathrm{B}}$ in the conventional case. The part of the Rh moment due to the Fe-Rh hybridization is thus almost two times larger than the one corresponding to the spin-dependent part of the exchange potential ($0.407\mu_{\mathrm{B}}$).

The Rh atom in B2-FeRh is surrounded by eight nearest Fe atoms. On the other hand, only four nearest Fe atoms are present in the disordered bcc-(Fe_{50},Rh_{50}) alloy on the average. We have obtained $m^{\mathrm{Fe}} = 2.820/2.789\mu_{\mathrm{B}}$ and $m^{\mathrm{Rh}} = 0.639/0.255\mu_{\mathrm{B}}$ for models with the conventional/suppressed exchange, respectively. The reduced Fe surrounding diminishes the induced Rh moment as expected, but even in this case a significant part of the moment is due to the Fe-Rh hybridization. The above calculations clearly demonstrate the relevance of the Fe-Rh hybridization for the formation of the Rh moment in the FM FeRh alloy.

B. Order-disorder transition

The parent lattice of the ordered B2 alloy is the bcc lattice. It therefore makes sense to investigate the order-disorder transition from the hypothetical disordered bcc-FeRh alloy into the ordered B2-FeRh alloy using the effective pair interactions. It is not the aim of this study to investigate a real structural transition from the fcc to B2 phases, but rather to understand processes in existing alloys. It is in the spirit of the construction of the Ising model (1) that one has to use related, not necessarily existing, alloys.

We have thus used as a reference state for estimation of the effective pair interactions V_{ij} the disordered bcc-($Fe_{0.5}$,$Rh_{0.5}$) alloy in the nonmagnetic phase using the GPM approach [19]. The lattice Fourier transform $V(\mathbf{q})$ of V_{ij} allows us to discuss the phase stability using the mean-field concentration-wave approach [18,19]. The minimum of $V(\mathbf{q})$ at the high-symmetry point $\mathbf{q}_{\mathrm{ord}}$ indicates an ordering tendency to form a superstructure compatible with it [18] while the minimum at $\mathbf{q}_{\mathrm{ord}} = 0$ corresponds to a segregation of alloy components. Results are shown in Fig. 3. Dominating positive V_{ij}'s for the first two nearest-neighbor pair interactions [Fig. 3(a)] indicate a clear ordering tendency in the alloy. The corresponding lattice Fourier transform $V(\mathbf{q})$ [Fig. 3(b)] has a pronounced minimum at $\mathbf{q}^{\mathrm{ord}} = 2\pi\ (1,0,0)/a$ (the high-symmetry point H in the bcc Brillouin zone) which confirms ordering to the B2 phase [18] compatible with the experimental data. An effective medium order-disorder temperature is $T_{\mathrm{ord}} = -V(\mathbf{q}^{\mathrm{ord}})/(4k_{\mathrm{B}})$ [18]. Calculated T_{ord} is about 1700 K in an acceptable agreement with the experimental value (1570 K) if one considers the well-known tendency of the mean-field approximation to overestimate T_{ord}.

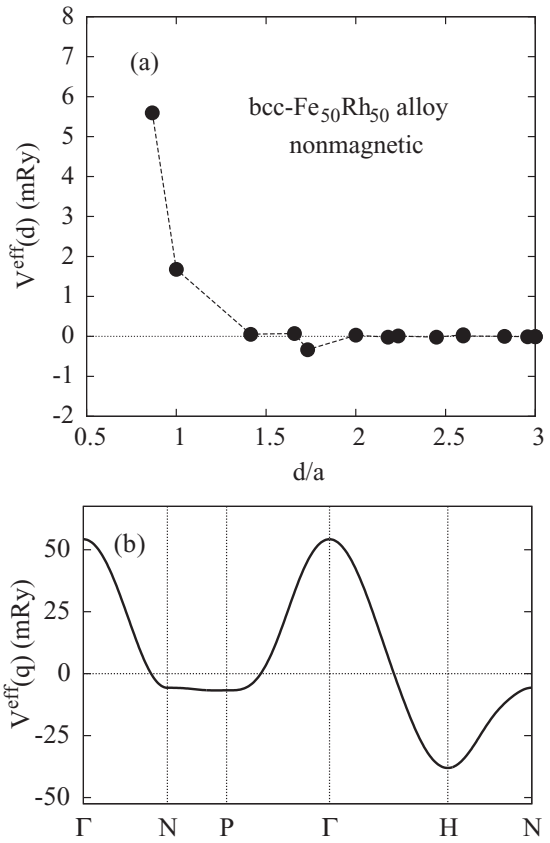

FIG. 3. (a) Effective pair interactions V_{ij} in the disordered nonmagnetic bcc-($Fe_{0.5}$,$Rh_{0.5}$) alloy as a function of the interatomic distance d in units of the lattice constant a, and (b) its corresponding lattice Fourier transform $V(\mathbf{q})$. The minimum of $V(\mathbf{q})$ at the ordering vector $\mathbf{q}_{\mathrm{ord}} = H$ indicates ordering to the B2 phase (the CsCl lattice type).

C. Exchange integrals

In this section, we wish to investigate character of exchange interactions in both the FM and AFM phases with the aim to identify interactions responsible for the FM to AFM transition. We will show that the same interactions relevant for the FM to AFM transition are already present in the B2 phase above the Curie temperature without any magnetic order.

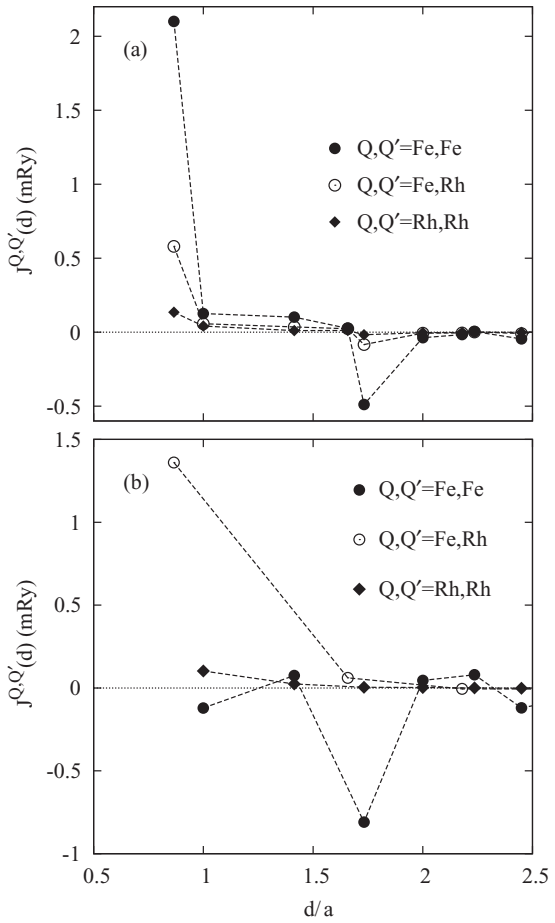

FIG. 4. The exchange interactions $J^{Q,Q'}$, $Q,Q' =$ Fe, Rh, as functions of the interatomic distance d (in units of the lattice parameter a) calculated in the disordered FM bcc-($Fe_{0.5}$,$Rh_{0.5}$) alloy (a) and the ordered FM B2-FeRh alloy (b).

1. FM reference state

The ordered FM B2-FeRh state exists below the order-disorder temperature. Nevertheless, it is instructive to show also interactions in the hypothetical disordered bcc phase. Results are shown in Figs. 4(a) and 4(b) for the disordered bcc-($Fe_{0.5}$,$Rh_{0.5}$) and the ordered B2-FeRh alloys, respectively. The main difference between both systems consists in the fact that in the B2 phase the first nearest-neighbors (NN) exchange interactions are Fe-Rh ones while the nearest Fe-Fe (and also the Rh-Rh) interactions are only the second NN interactions. In the disordered bcc phase, on the contrary, all types of interactions exist at any distance. The following conclusions can be made: (i) dominating Fe-Fe interactions $J^{\mathrm{Fe,Fe}}(\frac{1}{2},\frac{1}{2},\frac{1}{2})$ present in the bcc phase are missing in the B2 phase (Fe atoms are on a simple-cubic Fe sublattice). The exchange interactions among Rh atoms are small in both cases; (ii) important role of nearest-neighbor $J^{\mathrm{Fe,Rh}} = J^{\mathrm{Rh,Fe}}$ interactions between different atomic species in both bcc and B2 phases is seen. These interactions are crucial for the B2 phase, where they become dominating thus confirming their relevance for the formation of the ordered FM B2 phase. Results for the B2 phase are in a good agreement with those in Ref. [13]; and (iii) large AFM-like $J^{\mathrm{Fe,Fe}}(1,1,1)$ interactions, in particular in the ordered FM B2 phase (third NN ones), are a precursor of the AFM phase although they are clearly seen also in the disordered bcc phase. We have also calculated exchange interactions in the bcc DLM phase with total zero magnetic moment. In this case, only $J^{\mathrm{Fe,Fe}}$ are nonzero and they are essentially identical to those for the FM reference state (not shown). This result is in accord with Fig. 2, demonstrating the rigidity of Fe moments with respect to the spin rotations.

We have also calculated exchange interactions in the FM B2-FeRh, but now without exchange splittings on Rh atoms (see Sec. III A 3). In this case, $J^{\mathrm{Rh,Rh}}$ and, in particular, $J^{\mathrm{Fe,Rh}}$ exchange interactions are zero and the only nonzero ones are those among the Fe atoms. Although the character of $J^{\mathrm{Fe,Fe}}$ interactions remains the same as in FM B2-FeRh [Fig. 4(b)] or DLM B2-FeRh (Fig. 5) cases, namely, the dominating first NN and third NN AFM interactions, their magnitudes are more than two times larger. This result clearly proves the importance of exchange and correlations on the Rh atoms for the ferromagnetism of B2-FeRh alloys: without strongly ferromagnetic Fe-Rh interactions the system would be antiferromagnetic.

2. AFM and DLM reference states

The exchange interactions for the AFMII reference state are shown in Fig. 5. They are compared with interactions in the spin-disordered (paramagnetic) B2 DLM phase corresponding to the state above the Curie temperature (but below the order-disorder transition). The B2 DLM phase has completely disordered moments on the Fe sublattice and zero moments on the Rh sublattice. It should be noted that in the DLM phase there is no preference for the magnetic order (the high-temperature phase). On the contrary, in the AFMII

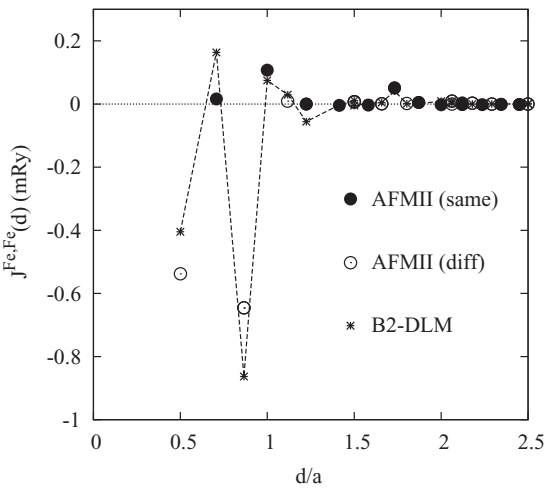

FIG. 5. The exchange interactions $J^{\mathrm{Fe,Fe}}$ as a function of the interatomic distance d calculated using different reference states: (i) the B2 DLM state (stars), and (ii) the ordered AFMII FeRh alloy. In the latter case, we distinguish between interactions among spins on the same Fe sublattice (filled circles, labeled as "same") and interactions between different magnetic Fe sublattices with opposite spin orientations (empty circles, labeled as "diff"), respectively. All interatomic distances are given in units of the AFMII lattice parameter a.

phase the spin arrangement is forced to correspond to the low-temperature ground state. The DLM and AFMII phases have both the total zero magnetization and an equal amount of spins pointing in opposite directions which, however, are ordered in the AFMII phase and completely disordered in the B2 DLM phase. We wish to make the following comments: (i) The local moments on Rh sites vanish in both cases so that $J^{Fe,Fe}$ interactions are the only nonzero ones. (ii) In the AFMII phase, we distinguish between Fe-Fe interactions on the same Fe sublattice and those between different Fe sublattices with oppositely oriented spins. The latter ones are predominantly AFM like. (iii) The most interesting result is that exchange interactions in the B2 DLM phase and the AFMII phase are very similar. (iv) The dominating $J^{Fe,Fe}(\frac{1}{2},0,0)$ (first NN) and $J^{Fe,Fe}(\frac{1}{2},\frac{1}{2},\frac{1}{2})$ (third NN) interactions in the DLM B2 phase seem to be responsible for the FM to AFM transition and they naturally correspond to interactions among Fe moments on different sublattices in the AFMII lattice. (v) Also, the $J^{Fe,Fe}$ interactions in the FM B2 phase [see Fig. 4(b), full circles] exhibit the same trend as $J^{Fe,Fe}$ interactions in the AFMII and DLM B2 phases, although their absolute values slightly differ due to different reference states. This demonstrates the robustness of Fe-Fe interactions even in the presence of local Rh moments.

In conclusion of this section, we wish to make two remarks: (i) The present approach gives a magnetization averaged over a given atomic cell. In the AFM state, the local Rh moment vanishes. The behavior of Rh magnetization inside the cell requires the full potential approach. This problem was discussed in Ref. [13] and it was demonstrated that the zero value of the Rh moment in the AFM state is in fact a result of the compensation of the opposite spin polarizations in different parts of Rh atomic cell. The authors of Ref. [13] argue that such implicit spin polarization of Rh atoms at low temperatures transforms into an explicit spin polarization of Rh atoms in the FM state. (ii) In general, the classical Heisenberg model for a system with strongly varying moment sizes (the Rh moment in the FeRh alloy) has to be modified for quantitative conclusions such as, e.g., the estimate of critical temperatures [13,14]. On the other hand, we made qualitative conclusions based on the representive FM and AFM phases where the Heisenberg description is applicable.

3. *Volume dependence of exchange integrals*

The study of the volume dependence of the exchange integrals gives an additional insight into their properties [13,14]. Different lattice constants can be realized, e.g., with help of samples grown by sputtering/molecular epitaxy on different substrates. The reduced/expanded volume leads to (i) larger/smaller overlap of wave functions, and (ii) increased/reduced bandwidths. The former effect enhances/reduces exchange integrals while the latter one reduces/enhances exchange integrals due to reduced/enhanced magnetic moments. The net values are thus competition of the above two effects.

In Fig. 6, we compare exchange integrals calculated for the AFMII reference state at ambient volume with those for reduced/expanded lattice parameters by about 5% each. Different volumes are expressed in terms of corresponding

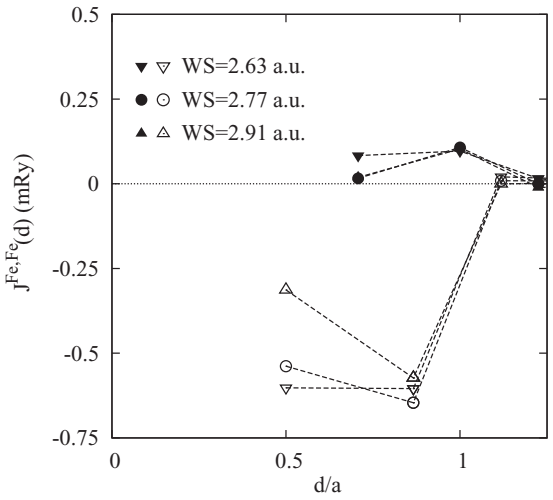

FIG. 6. The exchange interactions $J^{Fe,Fe}$ calculated for the AFMII reference state and for different lattice constants expressed in terms of corresponding Wigner-Seitz (WS) radii: (i) WS = 2.63 a.u., (ii) WS = 2.77 a.u. (experiment), and (iii) WS = 2.91 a.u. The full (empty) symbols correspond to interactions between the same (full symbols) and different (empty symbols) Fe sublattices.

Wigner-Seitz radii. The following conclusions can be done: (i) The volume dependence is stronger for exchange interactions among Fe atoms with opposite spins as compared to interactions among Fe atoms with parallel spins. (ii) The strength of dominating AFM interactions among Fe atoms with opposite spins is reduced/enhanced when the volume increases/decreases. In the light of discussion above, this means that their volume dependence is controlled by overlap of wave functions rather than by corresponding modifications of magnetic moments. (iii) The effect of volume is stronger when volume is expanded. It should be noted that a similar effect for expanded volume was obtained recently in Ref. [13] for the FM B2 phase although absolute values are slightly different due to different reference configurations. (iv) For the expanded volume, the ground state becomes the FM one while for the reduced volume the ground state is the AFMII. The stability of the AFMII state as compared to the FM state increases with reduced volume: it is 0.77 and 4.60 mRy/atom. These values agree with those of Ref. [4] although they are smaller. It should be noted that calculations in Ref. [4] are nonrelativistic and employ the fixed-spin moment approach constraining the total moment per unit cell. This result is also compatible with the experiment on the pressure dependence of the critical temperature for the AFMII to FM transition which increases linearly with pressure in the rate about 4.5 K/kbar [36].

D. Transport properties

In this section, we present results of transport studies in FeRh alloys, namely, the residual resistivity and the AMR ratio. We wish to concentrate on two interesting aspects: (i) the AMR, namely, its existence not only in the FM phase, but particularly also in the AFM one in connection with its potential use in spintronic applications [3], and (ii) the resistivity close to the FM-AFM phase transition, specifically on the large resistivity drop at the AFM to FM transition. A

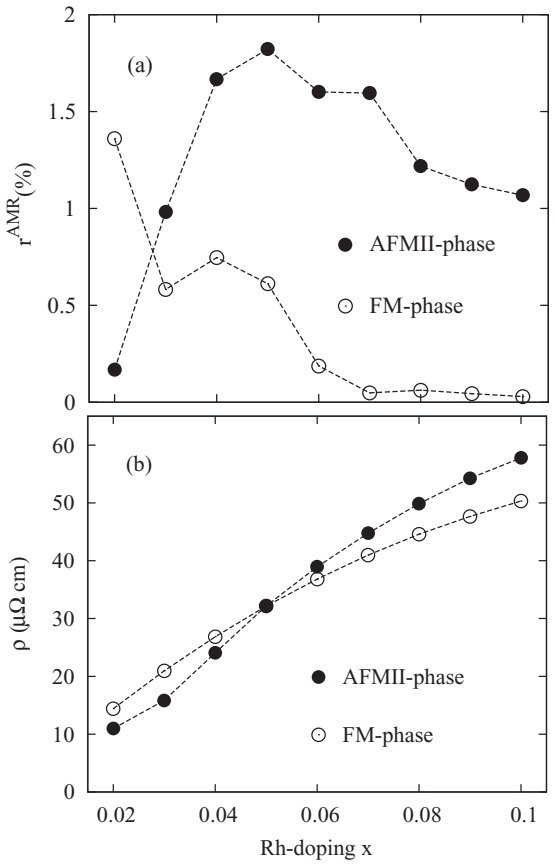

FIG. 7. The transport properties of the $(Fe_{1-x},Rh_x)Rh$ alloys in the AFMII and hypothetical FM phases both neglecting the temperature effect ($T = 0$ K): (a) the AMR ratios r^{AMR}, and (b) the residual resistivities.

relevant feature of this study is incorporation of the effect of finite temperature, although in an approximate way. We reiterate that the AFM to FM transition can be achieved either by temperature tuning or by applying or switching off the external magnetic field for temperatures slightly below the AFM to FM transition (the magnetic heating/cooling) [16,17].

1. Properties of magnetically ordered systems

In a recent pilot study [3] we have calculated the AMR ratio r^{AMR} (5) at the zero temperature for the AFMII phase as well as for the hypothetical FM phase to illustrate the effect. Two models were used: (i) a slightly off-stoichiometric FeRh alloy $(Fe_{1-x},Rh_x)Rh$ (Rh doping x is below 10%); such model has an experimental justification [3]. The model fully neglects the effect of temperature on the transport; and (ii) a finite-relaxation-time model applied to the ideal FeRh alloy in which temperature-dependent scattering due the phonons and magnons is modeled in a phenomenological manner by adding a finite Imz to the Fermi energy in transport equations.

The results are summarized in Fig. 7 for the model with Rh doping and in Table I for the finite-relaxation-time model, respectively. We mention that experiment for samples prepared by the molecular epitaxy method [3] gives r^{AMR} values in the range 0.1% to 1% and the resistivity in the AFM phase about 200 $\mu\Omega$ cm. Experiments performed on sputtered samples

TABLE I. Calculated residual resistivities ρ and values of the AMR ratio r^{AMR} (5) for the ideal stoichiometric FeRh alloy in the ferromagnetic (FM) and antiferromagnetic AFMII phases (AFM). The values of finite relaxation times which enter the theory through the imaginary part Imz (in Ry) added to the Fermi energy are shown. Resistivities are given in $\mu\Omega$ cm and r^{AMR} values in %. We also present the r^{AMR} values and resistivities calculated for enlarged (2.91 a.u.) and reduced (2.63 a.u.) Wigner-Seitz radii (the experimental Wigner-Seitz radius is 2.77 a.u.).

Imz	WS radius	r^{AMR} (AFM)	r^{AMR} (FM)	ρ (AFM)	ρ (FM)
10^{-3}	2.77	0.41	0.36	34	7
5.10^{-3}	2.77	0.37	0.40	113	29
10^{-2}	2.77	0.18	0.39	140	53
10^{-2}	2.91	0.19	0.42	162	67
10^{-2}	2.63	0.02	0.36	102	30

report resistivities about 65 and 125 $\mu\Omega$ cm in the FM and AFM, respectively, if the field cooling at the room temperature is used and resistivities about 150 and 270 $\mu\Omega$ cm for cooling from 385 to 350 K [16,17]. All results are sensitive to sample annealing, but a pronounced drop of resistivities through the transition from the AFM to FM phases seems to be firmly established.

The present results for residual resistivities of the FM and AFMII phases can be compared to previous calculations done in the scalar-relativistic limit and neglecting the transport vertex corrections (see Fig. 2 in Ref. [37]). The calculated magnetoresistance was due to different magnetic structure of the FM and AFMII phases rather than to relativistic effects which was the object of the study of Ref. [3]. Strictly speaking, the effect is similar to the giant magnetoresistance (GMR) studied in the past in metallic multilayers and it exists, contrary to the AMR effect, also in the scalar-relativistic limit. In fact, the B2-FeRh can be considered as a natural multilayer system [37]. The additional scattering due to spin-orbit effects which mixes up both spin channels leads to an enhancement of residual resistivities in the present relativistic case.

The r^{AMR} values calculated in both models are within experimental error bars. We have demonstrated [23] that the values of r^{AMR} in the FM Ni-based alloys depend on the disorder strength in the majority spin channel, with the highest r^{AMR} values obtained for alloys with negligible spin-up scattering. On the contrary, if disorder strengths in both channels are comparable, the r^{AMR} values are small. This seems to be also the present case which thus qualitatively explains small calculated and measured r^{AMR} values for FeRh. However, values of resistivities in the AFMII phase obtained for the Rh-doped FeRh alloy are too small as compared to experiment. Also, resistivities of the AFMII phase and of the hypothetical FM phase are very similar [see Fig. 7(b)], while in the experiment resistivities of the AFM and FM phases are very different. It should be noted that calculations in Rh-doped FeRh alloy for both phases correspond to the zero temperature. Essentially linear increase of residual resistivities with Rh concentration in both magnetic phases corresponds to the low-concentration limit in the Kubo-Greenwood transport equations (impurity concentration is up to 10%) [38]. Similar resistivities of the FM and AFMII phases are due to the

fact that impurity Rh atoms on Fe sublattices scatter roughly similarly for both spin orientations. One thus needs another and stronger scattering mechanism to obtain results compatible with experiment. We will demonstrate that it is the temperature which leads to scattering among differently oriented magnetic moments. Such scattering is particularly strong for oppositely oriented moments due to a large exchange splitting which manifests itself in large Fe-spin moments of order $3\mu_B$. The latter mechanism is included, although on an approximate level, in a simple finite-relaxation-time model which includes the effect of temperature empirically in terms of finite Imz and gives a pronounced resistivity drop as found in the experiment. Both models differ also in details concerning effect of disorder on the r^{AMR} values: while increasing chemical disorder leads to increasing values of the r^{AMR} for the AFM phase, the finite-relaxation-time model gives an opposite trend.

The effect of volume on transport properties is also illustrated in Table I using the finite-relaxation-time model with Im$z = 10^{-2}$ Ry. The resistivity increases/decreases with corresponding volume changes for both the FM and AFMII phases. While the relaxation time is fixed (Im$z = 10^{-2}$ Ry), the bandwidth decreases/increases for corresponding volume changes thus leading to relative increase/decrease of the scattering strength at the Fermi energy. The AMR ratios follow the same trend in both phases, namely, they increase/decrease for enlarged/reduced volumes. The spin-orbit effect in broader bands has to be weaker as compared to narrower bands, which is a rough explanation of the effect. The changes are rather small, with the exception of the dramatic decrease of the r^{AMR} value for AFM phase and reduced volume. While a decrease of the AMR ratio for broader bands is in accord with the above qualitative explanation, such large decrease is unexpected. We do not have a simple explanation for this fact, we have just checked that it is not caused by numerical inaccuracy or by an insufficient convergence with respect to the number of k points.

2. *Effect of spin disorder*

Keeping in mind the success of a simple finite-relaxation-time model, we proceed further to describe the effect of temperature in a more quantitative way. In particular, we wish to investigate the AFM to FM transition mediated by external field and its effect on transport properties [16]. This case is simplified by the fact that experiment is done at a fixed temperature and we shall thus concentrate on the effect of the spin disorder caused by temperature. The effect of spin disorder [32] is simulated in the framework of the uncompensated DLM (uDLM) model which was recently successfully applied to study the effect of temperature on transport properties in ordering Pd-rich PdFe and FePt alloys in the $L1_2$ and $L1_0$ structures, respectively [33,34]. The spin disorder is described as a random distribution of local moments $Fe^{[+]}$ and $Fe^{[-]}$ pointing in opposite directions. Formally, it can be described as a random ternary alloy $(Fe^{[+]}_{1-x-y}, Fe^{[-]}_{y}, Rh_x)$ on each Fe sublattice (we treat also FM phase in the AFMII lattice for an internal consistency). The amount of oppositely oriented Fe moments is y. This situation can be conveniently treated using the CPA. While the effect of temperature is correctly related to the amount of spin disorder in the system (characterized by the quantity y), a quantitative relation of y and the temperature is beyond limits of this model. It should be noted that the collinear CPA model for spin disorder [32] is an accurate mapping of the problem for temperatures at and above critical ones; its use for temperatures below the critical temperature is an additional, but acceptable approximation. A possible effect of phonons at a given temperature can be eventually simulated by adding a small finite Imz. In this case, the combined effect of spin and phonon disorders is treated beyond a simple Matthiessen rule [39].

We applied the uDLM to the Rh-doped ($x = 5\%$) FeRh alloy studied above for $T = 0$ K assuming that $y = 0.05$. This is a reasonable choice if one considers the temperature at which magnetic heating was done ($T =$ 300 K) and the Curie temperature ($T =$ 670 K) [33,34]. Calculated resistivities of the AFM and FM phases, 124.8 and 52.4 $\mu\Omega$ cm, respectively, compare well with the experiment (127 and 68 $\mu\Omega$ cm) [16]. The origin of a pronounced resistivity drop is thus strong disorder among oppositely oriented local moments on Fe sublattices in the AFMII phase which is missing in the FM phase. We remind that for the present Rh-rich case, resistivities at $T = 0$ K were similar being about 30 $\mu\Omega$ cm [see Fig. 7(b)]. The spin disorder thus enhances the FM resistivity by about 70%, but the AFM one by almost 420%.

In the case of the AFM phase we have also done calculations assuming $y = 0.03$, i.e., for the smaller spin disorder which corresponds in our simple model to a lower temperature. Calculated resistivity was reduced from 124.8 to 94.02 $\mu\Omega$ cm, which is the expected result. On the other hand, the AMR ratio has increased from the value of 0.06% for $y = 0.05$ to the value of 0.43% for $y = 0.03$.

We have also used the same model using the scalar-relativistic transport codes to see the effect of relativistic corrections. In this case, the AMR ratio is zero, but calculated AFM and FM resistivities are similar, being 122.2 and 33.5 $\mu\Omega$ cm for the AFM and FM phases, respectively. This confirms that the spin-disorder effects and not the relativistic effects are responsible for the large drop of resistivities during the AFM to FM phase transition.

The spin-disorder resistivity (SDR), which is the resistivity in the paramagnetic state above the Curie temperature, can be also estimated. This state can be reasonably represented using the DLM approach [40]. We give here the result for the ideal ordered B2 alloy which exists above the Curie temperature. The calculated value is 131.5 $\mu\Omega$ cm in the relativistic case and 107.8 $\mu\Omega$ cm in the scalar-relativistic limit. Larger resistivities in the relativistic case as compared to the scalar-relativistic one are caused by an additional scattering between the majority and minority spin channels due to the spin-orbit coupling.

It should be noted that in this section we have implicitly assumed the validity of the Matthiessen rule, namely, the fact that contributions from phonons and spin disorder are additive. It is not generally correct [39], but we have verified its validity in the present FeRh alloy by performing resistivity calculations for the AFMII FeRh alloy assuming (i) Im$z = 10^{-3}$ Ry without the spin disorder ($y = 0$), (ii) Im$z = 10^{-5}$ Ry with the spin disorder ($y = 0.05$), and (iii) Im$z = 10^{-3}$ Ry and the same spin disorder as in (ii). The finite Imz is a rough model of the disorder due to phonons (although there is no relation to a certain temperature). The corresponding resistivities are 34.2,

101.4, and 129.9 $\mu\Omega$ cm. The latter value compares very well with the Matthiessen's rule resistivity of 135.6 $\mu\Omega$ cm.

It should be mentioned that a more sophisticated way of the estimation of temperature effects on the resistivity has been proposed recently [41,42] in which the supercell Landauer-Büttiker formulation of the resistivity combined with the Monte Carlo simulations of phonon and spin disorders was used. But, even such approach has a limitation due to the use of the classical (Monte Carlo) versus quantum statistics, the latter being relevant for low-temperature behavior of magnons.

IV. CONCLUSIONS

We have presented, based on the unified first-principles model (the relativistic TB-LMTO approach), estimates of a broad range of physical properties of FeRh alloys. The main results can be summarized as follows: (i) The magnetic moments agree with experiment as well as with other theoretical approaches and their values are influenced by relativistic effects only weakly. (ii) Sizes of the local Rh moments are very sensitive to their relative orientations with respect to the Fe moments whose sizes remain essentially unchanged. This result demonstrates the relevance of induced Rh moments for ferromagnetism of the FeRh and can also qualitatively describe the AFM to FM transition in which Rh moments missing in the AFM phase appear in the FM one. (iii) The magnetic Rh moments in the FM state are predominantly due to the hybridization with surrounding polarized nearest-neighbor Fe atoms rather than due to the spin-dependent part of the exchange-correlation potential. (iv) Pair chemical interactions clearly indicate the ordering tendency in random bcc-$(Fe_{0.5},Rh_{0.5})$. We have shown that the CsCl lattice develops from the hypothetical disordered bcc phase on cooling and that the estimated mean-field order-disorder temperature is in a fair agreement with the experiment. (v) Detailed analysis of magnetic exchange interactions in various reference states has allowed us to understand more details concerning the FM to AFM transition. In particular, large AFM-like $J^{\mathrm{Fe,Fe}}(1,1,1)$ interactions in the FM B2 phase are a precursor of the transition to AFM phase and they are also seen even in the disordered bcc phase. (vi) The large resistivity drop at the phase transition from the AFM to FM phase can be understood only by invoking the effect of temperature on the transport. In particular, we have found a relevant effect of large spin disorder between Fe sublattices in the AFM phase which is missing in the FM phase. This was demonstrated using both a simple finite-relaxation-time model and the uncompensated DLM model which simulates the temperature-induced spin disorder more realistically.

ACKNOWLEDGMENT

The authors acknowledge support from Czech Science Foundation (Grant No. 14-37427G).

[1] O. Kubaschewski, *Iron-Binary Phase Diagrams* (Springer, Berlin, 1982).
[2] G. Shirane, R. Mathans, and C. W. Chen, Phys. Rev. **134**, A1547 (1964).
[3] X. Marti, I. Fina, C. Frontera, Jian Liu, P. Wadley, Q. He, R. Paull, J. Clarkson, J. Kudrnovský, I. Turek, J. Kuneš, D. Yi, J.-H. Chu, C. T. Nelson, L. You, E. Arenholz, S. Salahuddin, J. Fontcuberta, T. Jungwirth, and R. Ramesh, Nat. Mater. **13**, 367 (2014).
[4] V. L. Moruzzi and P. M. Marcus, Phys. Rev. B **46**, 2864 (1992).
[5] J. B. Staunton, Rep. Prog. Phys. **57**, 1289 (1994).
[6] S. Yuasa, H. Miyajima, Y. Otani, and A. Sakuma, J. Magn. Magn. Mater. **140–144**, 79 (1995).
[7] A. Jezierski and G. Borstel, J. Magn. Magn. Mater. **140–144**, 81 (1995).
[8] J. Kübler, *Theory of Itinerant Electron Magnetism* (Oxford University Press, Oxford, 2000).
[9] P. M. Derlet, Phys. Rev. B **85**, 174431 (2012).
[10] M. E. Gruner, E. Hoffmann, and P. Entel, Phys. Rev. B **67**, 064415 (2003).
[11] R. Y. Gu and V. P. Antropov, Phys. Rev. B **72**, 012403 (2005).
[12] O. N. Mryasov, Phase Trans. **78**, 197 (2005).
[13] L. M. Sandratskii and P. Mavropoulos, Phys. Rev. B **83**, 174408 (2011).
[14] A. Deák, E. Simon, L. Balogh, L. Szunyogh, M. dos Santos Dias, and J. B. Staunton, Phys. Rev. B **89**, 224401 (2014).
[15] J. B. Staunton, R. Banerjee, M. dos Santos Dias, A. Deak, and L. Szunyogh, Phys. Rev. B **89**, 054427 (2014).
[16] M. A. de Vries, M. Loving, A. P. Mihai, L. H. Lewis, D. Heiman, and C. H. Marrows, New J. Phys. **15**, 013008 (2013).
[17] I. Suzuki, T. Naito, M. Itoh, T. Sato, and T. Taniyama, J. Appl. Phys. **109**, 07C717 (2011).
[18] F. Ducastelle, *Order and Phase Stability in Alloys* (North Holland, Amsterdam, 1991).
[19] J. Kudrnovský, I. Turek, A. Pasturel, R. Tetot, V. Drchal, and P. Weinberger, Phys. Rev. B **50**, 9603 (1994).
[20] A. I. Liechtenstein, M. I. Katsnelson, V. P. Antropov, and V. A. Gubanov, J. Magn. Magn. Mater. **67**, 65 (1987).
[21] I. Turek, J. Kudrnovský, V. Drchal, and P. Bruno, Philos. Mag. **86**, 1713 (2006).
[22] I. Turek, J. Kudrnovský, V. Drchal, L. Szunyogh, and P. Weinberger, Phys. Rev. B **65**, 125101 (2002).
[23] I. Turek, J. Kudrnovský, and V. Drchal, Phys. Rev. B **86**, 014405 (2012).
[24] The DLM state corresponds to the magnetic state with spins oriented randomly in each direction with the same probability and with the zero total moment. The problem can be formally mapped onto the random equiconcentration alloy with spins pointing up and down and corresponding self-consistent magnetic moments can be thus determined using the CPA. See, for details, B. L. Gyorffy, A. J. Pindor, J. Staunton, G. M. Stocks, and H. Winter, J. Phys. F: Met. Phys. **15**, 1337 (1985).
[25] A. B. Shick, V. Drchal, J. Kudrnovský, and P. Weinberger, Phys. Rev. B **54**, 1610 (1996).
[26] O. K. Andersen and O. Jepsen, Phys. Rev. Lett. **53**, 2571 (1984).
[27] I. Turek, V. Drchal, J. Kudrnovský, M. Šob, and P. Weinberger, *Electronic Structure of Disordered Alloys, Surfaces and Interfaces* (Kluwer, Boston, 1997); I. Turek, J. Kudrnovský, and V. Drchal, in *Electronic Structure and Physical Properties of*

Solids, edited by H. Dreyssé, Lecture Notes in Physics Vol. 535 (Springer, Berlin, 2000), p. 349.
[28] S. H. Vosko, L. Wilk, and M. Nusair, Can. J. Phys. **58**, 1200 (1980).
[29] J. W. D. Connolly and A. R. Williams, Phys. Rev. B **27**, 5169 (1983).
[30] K. Carva, I. Turek, J. Kudrnovský, and O. Bengone, Phys. Rev. B **73**, 144421 (2006).
[31] P. Czaja, F. Freimuth, J. Weischenberg, S. Blügel, and Y. Mokrousov, Phys. Rev. B **89**, 014411 (2014).
[32] J. Kudrnovský, V. Drchal, S. Khmelevskyi, and I. Turek, Phys. Rev. B **84**, 214436 (2011).
[33] J. Kudrnovský, V. Drchal, and I. Turek, J. Supercond. Nov. Magn. **26**, 1749 (2013).
[34] J. Kudrnovský, V. Drchal, and I. Turek, Phys. Rev. B **89**, 224422 (2014).
[35] S. Mirbt, A. M. N. Niklasson, B. Johansson, and H. L. Skriver, Phys. Rev. B **54**, 6382 (1996).
[36] R. C. Wayne, Phys. Rev. **170**, 523 (1968).
[37] I. Turek, J. Kudrnovský, V. Drchal, P. Weinberger, and P. H. Dederichs, J. Magn. Magn. Mater. **240**, 162 (2002).
[38] B. Velický, Phys. Rev. **184**, 614 (1969).
[39] J. K. Glasbrenner, B. S. Pujari, and K. D. Belashchenko, Phys. Rev. B **89**, 174408 (2014).
[40] J. Kudrnovský, V. Drchal, I. Turek, S. Khmelevskyi, J. K. Glasbrenner, and K. D. Belashchenko, Phys. Rev. B **86**, 144423 (2012).
[41] A. L. Wysocki, R. F. Sabirianov, M. van Schilfgaarde, and K. D. Belashchenko, Phys. Rev. B **80**, 224423 (2009).
[42] R. Kováčik, P. Mavropoulos, D. Wortmann, and S. Blügel, Phys. Rev. B **89**, 134417 (2014).